Synthesis of $MAPbBr_{3-i}Y_i$ (Y=I, Cl and i=0, 1, 2, 3) thin films perovskites

Erika Vega [*], Miguel Mollar[**], and Bernabé Marí[***]

Institut de Fabricació (IDF), Universitat Politècnica de València, Camí de Vera s/n, 46022, València, Spain

Received ZZZ, revised ZZZ, accepted ZZZ
Published online ZZZ (Dates will be provided by the publisher.)

Keywords Hybrid perovskites, Metilammonium lead halide, Optical absorption, Photoluminescence.

* e-mail ervefl@etsid.upv.es, Phone: +34 963 877 525
** e-mail mmollar@fis.upv.es, Phone: +34 963 877 525, Fax: +34 963 877 189
*** Corresponding author: e-mail bmari@fis.upv.es, Phone: +34 963 877 525, Fax: +34 963 877 189

Methylammonium lead halide perovskites with different halides (iodide, bromide and chloride) have been synthetized from methylamine, lead nitrate and the corresponding hydroX acid (X= I, Br, Cl) precursors. Subsequently $MAPbBr_{3-i}Y_i$ (Y=I, Cl; i=0, 1, 2, 3) perovskites were deposited as thin films onto FTO substrates by spin coating or dipping. Thin film perovskites were then characterized by X-Ray Diffraction, elemental analysis and optical spectrometry. Crystallites' sizes are between 100-600 nm depending on the synthesis temperature. All synthetized $MAPbX_{3-i}Y_i$ perovskites crystallized in the same cubic phase irrespective of the X and Y components and a unique phase is observed. Elemental analysis shows that in all cases the atomic components meet the expected stoichiometric formulae. The bandgap of thin film $MAPbX_{3-i}Y_i$ perovskites were inferred from transmittance and reflectance spectral measurements. It is found that the onset of the absorption edge for thin film $MAPbX_3$ perovskites is about 1.66, 2.55 and 3.37 eV for X= I, Br, Cl, respectively and it reaches intermediate values for mixed $MAPbX_{3-i}Y_i$ perovskites.

$MAPbX_3$ (X=I, Br, Cl) perovskite powders

1 Introduction Organolead halide perovskite materials as light absorbers have widened the horizons of high efficiency solid-state solar cells [1-4]. The generic structure of this perovskites is $APbX_3$ (A = cationic organic molecules; X = halides), being one of the main features of these compounds its abundance and low-cost. Due to their great absorption coefficient and high charge carrier mobility this group of perovskites are well suited for converting solar energy [5, 6]. As a result lead halide perovskites are having an important impact in the field of thin film photovoltaics in the last years boosting up energy conversion efficiency from 3.8% in 2009 [1] up to the present record of 20.1% reported by KRICT [7].

Very recently, many studies have been published focusing on material properties directly related to device performance, such as carrier mobilities, recombination lifetimes, excitonic properties and optical absorption [8].

Apart from the pure lead halide perovskites, the so called mixed halide perovskite have also been used for photovoltaic applications, in which the iodine is replaced partly with chlorine $CH_3NH_3PbI_{3-x}Cl_x$ [9, 10] which is derived from the pure halide perovskite $CH_3NH_3PbI_3$ via apical substitution of the iodine atom with a chlorine atom. The main challenge of the mixed halide perovskites is to improve the stability of these iodine-based materials.

Perovskite materials, known to be inexpensive and efficient at converting light to electricity, can also be used to

build light emitters. The emission properties of organolead halide perovskite materials make them very efficient and several emitter devices based on perovskites have already been demonstrated [11]

As an example, it has been demonstrated that crystalline $CH_3NH_3PbI_{3-x}Cl_x$ films obtained by solution processing can convert 70% of absorbed light into emitted light [12]. This remarkably high luminescent efficiency is critical for light-emitting devices and reference 12 reports the operation of an optically pumped vertical cavity laser comprising a layer of perovskite between a dielectric mirror and an evaporated gold top mirror.

Recently ultra-stable amplified spontaneous emission for solution-processed organic-inorganic perovskites ($CH_3NH_3PbX_3$ where X= Cl, Br, I) has also been reported [13]. This new capability of perovskites paws the way for the realization of on-chip coherent light sources. In fact reference 13 reports laser-light emission from perovskite crystals consisting of two-dimensional layers of metal halides separated by organic materials.

It is worth noting that organolead halide perovskites, $MAPbBr_{3-x}Cl_x$ have a larger band gap than other perovskites based on iodine and have been used in photovoltaic applications as light absorbers for high energy photons [14]. $MAPbBr_{3-x}Cl_x$ materials also exhibited strong PL intensities. The PL emission intensity and the average recombination lifetime strongly depend on the Br:Cl ratio. The longest recombination lifetime of 446 ns was found for $MAPbBr_{2.4}Cl_{0.6}$ while the strongest PL intensity was found for $MAPbBr_{2.25}Cl_{0.75}$ [8].

Depending on the excitation these solution-processed crystalline films of organolead mixed halides exhibited moderate to high PL quantum efficiencies at room temperature. This decreasing on the PL efficiency at low excitation density has been attributed to the presence of defects causing non-radiative decay and at high excitation density the defects were filled and radiative recombination became dominant [15].

The emission of mixed halide perovskite with Br and Cl ($CH_3NH_3PbBr_{3-x}Cl_x$) perovskite semiconductor has been tuned from 2.42 to 3.16 eV allowing the construction of light emitting diodes operating at room temperature and emitting in green and blue ranges [16].

However, despite the outstanding photovoltaic and emission performances that have been obtained using $MAPbI_3$ and its related mixed perovskites, the formation of mixed halide perovskites remains poorly investigated.

Here we report an investigation on pure $CH_3NH_3PbX_3$ (X= I, Br, Cl) perovskites and their related Br/I and Br/Cl mixed halide lead methylammonium perovskites. Pure I, Br and Cl lead methylammonium perovskites were synthetized from suitable solutions and then mixed perovskites were obtained by mixing pure perovskites in proper proportions. The halide ratio in the thin film perovskites follows the same ratio used in liquid precursors.

We present a study of their crystalline structure as well as the relationship between the absorption and emission of pure and mixed halides perovskites as a function of the Br:I and Br:Cl ratio in the material. We found out that the exact composition of the final compound reproduces the stoichiometry of the precursor solution. Therefore the optical absorption and emission properties can be optimized through composition tuning.

The photoluminescence properties and the recombination behaviour of the solution processed $MAPbBr_{3-i}Y_i$ (Y= I, Cl) (i=0, 1, 2, 3) thin films depend on different ratios of Br:I and Br:Cl.

2 Experimental

2.1 Synthesis of pure perovskite powders $MAPbX_3$ ($X = I,\ Br,\ Cl$) perovskite crystal powders were synthesized by mixing an equimolar ratio of 0.30 mol of CH_3NH_2 (33% in methanol from Sigma Aldrich) and hydrohalide acid HX ($X = I,\ Br,\ Cl$). The mixture was stirred for 2 hours in a 250 mL round-bottom flask, which was kept in an ice bath (0 ºC). Subsequently, this mixture was heated up to 100ºC for 30 minutes and then a solution of 0.030 mol of $Pb(NO_3)_2$ previously dissolved in 50 mL of distilled water was added drop-wise to the hot $CH_3NH_3X_3$ (X= I, Br, Cl) solution under vigorous stirring. After this process a precipitate of crystalline powders with different colours (black for iodide, orange for bromide and white for chloride) takes place. The remaining solution was then left to cool until 40ºC and filtered. The crystalline powders were washed several times with absolute ethanol, diethyl ether and then dried under vacuum. In particular $MAPbI_3$ powders were filtered on vacuum with the solution above 40ºC to avoid decomposition [17]. The synthesis described before obeys the following equation:

$$CH_3NH_2 + 3HX + Pb(NO_3)_2 \rightarrow CH_3NH_3PbX_3 + 2NO_3^- + 2H^+$$

2.2 Synthesis of thin film perovskites Iodine and bromine crystalline powders were dissolved at 45% wt in Dimethylformamide (DMF) solution and chloride perovskite was dissolved in Dimethylsulfoxide (DMSO).

The different mixed halide of perovskites $MAPbBr_{3-i}Y_i$ ($Y = I, Cl$ and $i = 0, 1, 2, 3$) were prepared by mixing the respective pure precursor solutions $MAPbX_3$ ($X = I, Br, Cl$) at 45% wt in the ratios 1:2 and 2:1, respectively. All solutions, three for pure perovskite and four for mixed halide perovskites were then deposited onto FTO substrates by spin coating or by dipping. Mixed perovskite containing iodides and chlorides were not considered in this study.

2.3 Characterization The perovskite thin films were characterized by X-Ray Diffraction using a RIGAKU Ultima IV in the Bragg-Bentano configuration using Cu Ka radiation.

Photoluminescence (PL) spectra were recorded at 10 K using a He-closed cryostat. The PL excitation source was a He-Cd laser emitting at 325 nm. Photoluminescence data were recorded by a Si-based CCD detector Hamamatsu.

Optical measurements were performed at room temperature using a spectrometer Ocean Optics HR4000 equipped with a Si-CCD detector. An integrating sphere was used to collect both specular and diffuse transmittance. The absorptance spectra were deduced from transmittance measurements.

3 Results and discussion Figure 1.a shows the X-Ray diffractograms for MAPbI3 and MAPbBr3 thin films and the combinations with iodine (MAPbI2Br and MAPbIBr2). All thin film diffractograms correspond to the same cubic structure corresponding to the spatial group labelled as P432 (207). The most intense diffraction peak located below 15 degrees corresponds to (1 0 0) diffraction planes and the peaks located at about 20, 30 and 34 degree are related to (1 1 0), (2 0 0) and (2 1 0) diffraction planes, respectively. Two diffraction peaks corresponding to FTO substrates and located 26.5 and 33.7 degrees are also observed.

All perovskite thin films, including pure and mixed halides, display the same cubic structure but the position of the peaks shifts according to the halide component and content in the thin film. The trend is the higher the average size of the halides in the perovskite the lower the position of the diffraction peak.

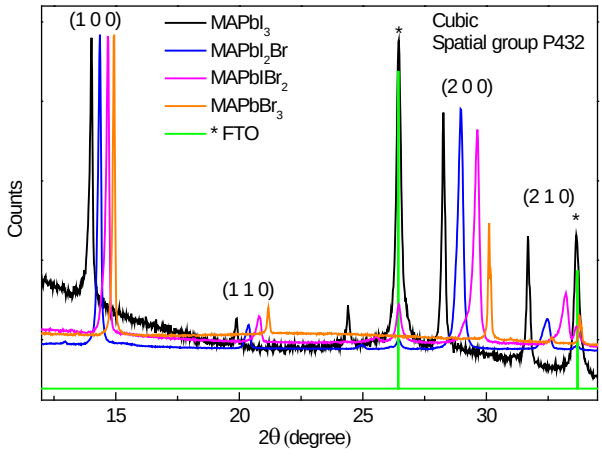

Figure 1.a X-Ray diffractogram for $MAPBI_iBr_{3-i}$ (i=0, 1, 2, 3) thin film samples.

Figure 1.b shows the X-Ray diffractograms for pure $MAPbBr_3$ and $MAPbCl_3$ thin films and their corresponding mixtures $MAPbBr_2Cl$ and $MAPbBrCl_2$. The intensity of XRD peaks has been normalized for the intensity of the most intense (0 0 1) peak. Again all pure and mixed Br and Cl organolead perovskites thin films exhibit cubic structure belonging to the spatial group P432. As for Br and I pure and mixed organolead perovskites the position of the diffraction peaks shifts to higher angles when the average size of halides contained in the thin film decreases, which means that the distance between diffraction planes is reduced due to the lower average size of halides.

The lattice constants were calculated by fitting the whole pattern using JADE software. It was found the lattice constant follows the called Vegard's law [18], which states that lattice constants vary linearly with the ratio between the two halides components of the thin films.

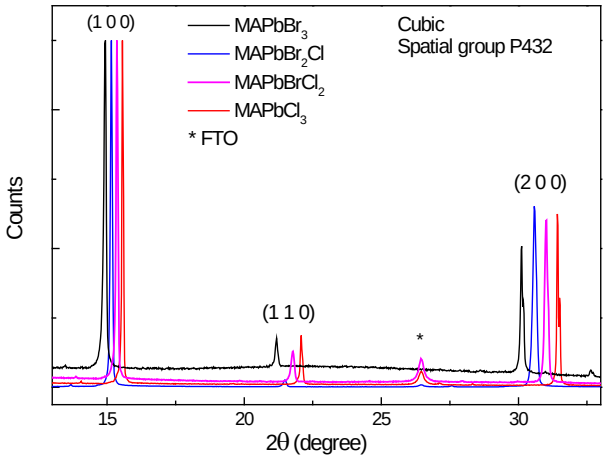

Figure 1.b X-Ray diffractogram for $MAPBr_iCl_{3-i}$ (i=0, 1, 2, 3) thin film samples.

Concerning the iodide and chloride mixed halide perovskite we were not able to synthetized layers with the same I:Cl ratio as we did for Br:I and Br:Cl mixed halides. In all attempts to synthetize $MAPbI_{3-i}Cl_i$ thin films the Cl content was very low, far away from the desired 1:2 or 2:1 ratios. This result agrees with the literature. It has been demonstrated experimentally and theoretically that the formation of continuous solid phase $MAPbI_{3-i}Cl_i$ is actually not alloyed and that chloride incorporation into $MAPbI_3$ is possible only at relatively low concentration, so that it could be classified as a dopant agent rather than alloy [19].

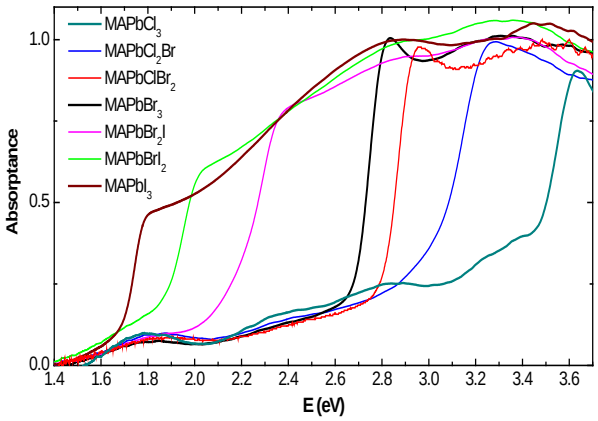

Figure 2 Absorptance for $MAPbBr_{3-i}Y_i$ (Y=I, Cl; i=0 ,1 ,2 ,3) thin film perovskites

Figure 2 shows the absorptance for $MAPbX_3$ (X=I, Br, Cl) thin film perovskites and the thin film mixtures $MAPbBrI_2$, $MAPbBr_2I$, $MAPbBrCl_2$, $MAPbBr_2Cl$. The main features of the absorption spectra are the existence of sub band gap absorption tail followed by a strong rise of the absorption, which corresponds to excitonic absorption, and then a transition from the valence band to the conduction band. When excitonic absorption dominates the absorption spectrum the classical relationship between the absorption coefficient (α) and the band gap energy (E_g) commonly used for calculating the bandgap of a direct semiconductor

$$(\alpha E)^2=A(E-E_g) \quad (1)$$

where E is the photon energy and A is a constant, is not longer valid and the Elliott's equation has to be used [20]. The different widths exhibited for the different perovskites difficult the calculation of the real bandgap, so in this paper we will refer the onset of the absorption edge. The absorption edge ranges from the lowest value (1.66 eV) for $MAPbI_3$, increases when decreasing the average size of the halides contained in the film, and reaches its highest value (3.37 eV) for $MAPbCl_3$. As expected the lower size of the halogen anion in the perovskite thin films results in a shift of the absorption edge to higher energies.

The sub band absorption exhibited for most perovskite thin films studied here could be related to optical transitions between the conduction or valence bands and energy levels located inside the gap or to the incomplete coating of the substrate by the perovskite thin films deposited by spin coating. An incomplete coating of the substrates is equivalent to the presence of voids in the films and should be observed in the transmittance spectra. However, this possibility cannot be inferred from the transmittance spectra, therefore we believe that the sub band gap absorption is related to transition involving intra gap energy levels. This hypothesis agrees with the featured observed for the photoluminescence spectra.

Table 1 displays the absorption edge at room temperature for the different perovskites in energy and in wavelength. These values were calculated from the onset of the absorptance shown in Figure 2.

Table 1 Absorption edge for $MAPbBr_{3-i}X_i$ (X= I, Cl) (i=0, 1, 2, 3) perovskite thin films.

Perovskite Composition	Absorption edge at 300K	
	(eV)	(nm)
$MAPbCl_3$	3.37	368
$MAPbCl_2Br$	2.95	420
$MAPbClBr_2$	2.77	448
$MAPbBr_3$	2.65	468
$MAPbBr_2I$	2.10	590
$MAPbBrI_2$	1.81	685
$MAPbI_3$	1.66	746

Figure 3 shows the photoluminescence spectra for the different mixtures of $MAPbX_3$ (X=I, Br, Cl) thin film perovskites and the $MAPbX_2Y$ (X=I, Br, Cl) and (Y=I, Cl) thin film mixtures considered in this work.

Again the energy of PL emission depends on the halide components of the thin film, ranging all the wavelengths of the visible spectrum. The lowest energy (highest wavelength (790 nm) is observed for $MAPbI_3$ sample while the highest energy and therefore lowest wavelength (398 nm) is observed for $MAPbCl_3$. The wavelength position for $MAPbBr_3$ yields in the middle (550 nm).

In most cases the shape of the photoluminescence spectra contains several peaks, which means that, apart from inter band transitions, other radiative transitions between the valence and/or conduction bands and some energy levels located inside the band gap are involved. The component of PL spectra with the highest energy corresponds to transitions from the conduction band to the valence band and the lower energy components of the PL spectra involve energy levels inside the band gap, which is in agreement with the sub band gap absorption mentioned before.

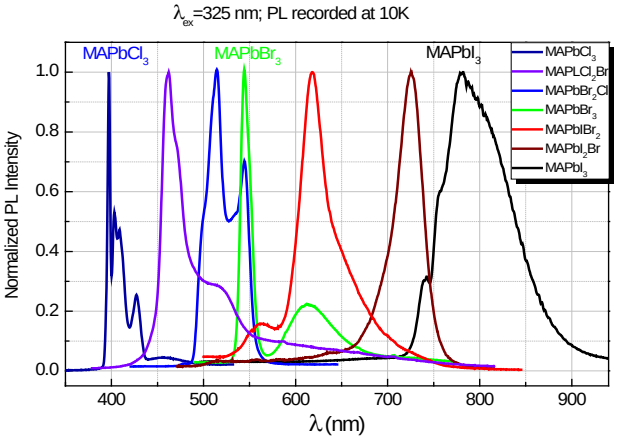

Figure 3 Photoluminescence spectra for $MAPbBr_{3-i}Y_i$ (Y=I, Cl; i=0 ,1 ,2 ,3) thin films recorded at 10 K.

The wavelength position of the maximum of the photoluminescence emission is always shifted to higher wavelengths when compared with the inset of the absorption edge.

The high intensity of PL emission suggests that most decay transitions are radiative and nonradiative decay is negligible. Since the radiative recombination dominates one can speculate that most energy levels inside the band gap correspond to shallow levels and electron-hole pairs formed during optical excitation recombine radiatively emitting photons. The amount of deep levels inside the bandgap is very low and as a result both pure and mixed perovskites exhibit high luminescent efficiency.

Table 2 show the energy position and related wavelength for the most intense PL peaks for the different $MAPbBr_{3-i}Y_i$ (Y= I, Cl and i=0, 1, 2, 3) perovskite thin films. The energy position of PL peaks is always red shifted with respect to the onset of the absorption edge.

Table 2 Position of the most intense PL peaks for organolead pure and mixed halide perovskites thin films recorded at 10K.

Perovskite Composition	PL peak position at 10K (eV)	(nm)
$MAPbCl_3$	3.11	398
$MAPbCl_2Br$	2.68	462
$MAPbClBr_2$	2.41	514
$MAPbBr_3$	2.27	544
$MAPbBr_2I$	2.00	618
$MAPbBrI_2$	1.71	725
$MAPbI_3$	1.58	780

4 Conclusion Methylammonium lead halide perovskites with different halides (iodide, bromide and chloride) and methylammonium lead halides mixtures (Br:I and Br:Cl), prepared by mixing pure methylammonium lead halide perovskites in the desired proportions, were synthetized from methylamine, lead nitrate and the corresponding hydroX acid (X= I, Br, Cl) precursors and deposited as thin films onto FTO substrates by spin coating or dipping.

All synthetized $MAPbBr_{3-i}Y_i$ (Y= I, Cl and i=0, 1, 2, 3) perovskites reported in this paper crystallized in the same cubic phase irrespective of the X component and the i-value and a unique spatial group P432 was observed. Furthermore, all synthetized organolead mixed halide thin film perovskites reached the expected stoichiometric as inferred from elemental analysis. In perovskite mixed halides combining I and Cl the chloride content was so low that should be considered as a dopant agent rather than a mixture.

The absorption edge of thin film perovskites can be tuned all along the visible spectrum from 368 to 746 nm. The bandgaps of thin film $MAPbX_{3-i}Yi$ perovskites were inferred from transmittance spectral measurements. It is found that the bandgap for thin film $MAPbX_3$ perovskites is about 1.66, 2.65 and 3.37 for X= I, Br, Cl, respectively and reaching intermediate values for mixed $MAPbX_{3-i}Y_i$ perovskites.

Low temperature PL emission can also be tuned along the visible spectrum from 400 to 800 nm. PL emissions are centred at 1.58, 2.27 and 3.11 eV for $MAPbI_3$, $MAPbBr_3$ and $MAPbCl_3$, respectively. PL emission energies for mixed halides perovskites are located in intermediate values. As a general rule it was observed that the centre of the PL emission at 10K is red shifted with respect the absorption edge measured at room temperature.

Acknowledgements This work was supported by Ministerio de Economía y Competitividad (ENE2013-46624-C4-4-R).

References

[1] A. Kojima, K. Teshima, Y. Shirai and T. Miyasaka, J. Am. Chem. Soc., **131**, 6050 (2009).

[2] H. S. Kim, C. R. Lee, J. H. Im, K. B. Lee, T. Moehl, A. Marchioro, S. J. Moon, R. Humphry-Baker, J. H. Yum, J. E. Moser, M. Gratzel and N. G. Park, *Sci. Rep*., **2**, 591, (2012).

[3] M. M. Lee, J. Teuscher, T. Miyasaka, T. N. Murakami and H. J. Snaith, *Science*, **338**, 643 (2012).

[4] B. Cai, Y. D. Xing, Z. Yang, W. H. Zhang and J. S. Qiu, *Energy Environ. Sci.*, **6**, 1480 (2013).

[5] N.G. Park, *J. Phys. Chem. Lett.*, **4**, 2423 (2013).

[6] H. J. Snaith, *J. Phys. Chem. Lett.*, **4**, 3623 (2013).

[7] http://www.nrel.gov/ncpv/images/efficiency_chart.jpg

[8] M. Zhang, H.Yu, M. Lyu, Q. Wang, J.H. Yun and L. Wang, *Chem. Commun*. **50**, 11726 (2014).

[9] J.You, Z. Hong, Y. M. Yang, Q.Chen, M. Cai, T. B. Song, C.C. Chen, S. Lu, Y. Liu, H. Zhou, and Y. Yang, *ACS Nano*, **8**, 1674 (2014).

[10] J. M. Ball, M. M. Lee, A. Hey, and H. J. Snaith, *Energy environ. Sci*. **6**, 1739 (2013).

[11] S.A. Bretschneider, J. Weickert, J.A. Dorman, and L. Schmidt-Mende, *APL Mater*. **2**, 040701 (204).

[12] F. Deschler, M. Price, S. Pathak, L.E. Klintberg, D. Jarausch, R. Higler, S. Hüttner, T. Leiitens, S.D. Stranks, H. J. Snaith, M. Atatüre, Richard T. Phillips, and R. H. Friend, *J. Phys. Chem. Lett.* **5,** 1421 (2014).

[13] G. Xing, N. Mathews, S.S. Lim, N. Yantara, X. Liu, D. Sabba, Dharani, M. Grätzel, S. Mhaisalkar, T.C. Sum, Low-temperature solution-processed wavelength-tunable perovskites for lasing, Nat Mater **13,** 1476 (2014).

[14] E. Edri, S. Kirmayer, D. Cahen, and G. Hodes, *J. Phys. Chem. Lett*. **5**, 429 (2013).

[15] S.G. Carrero, R.E. Galian, J.P. Prieto, *J. Mater. Chem. A*, **3**, 9187 (2015).

[16] K.L. Narasimhan, D.Kabra, *ACS Appl. Mater. Interfaces,* DOI: 10.1021/acsami.5b02159 (2015)

[17] D. Weber, *Z. Naturforch* 1443 (1978).

[18] L. Vegard (1921). *Zeitschrift für Physik* **5,** 17 (1921).

[19] S. Colella, E. Mosconi, P. Fedeli, A.a Listorti, F. Gazza, Fabio Orlandi, P.Ferro, T. Besagni, A. Rizzo, G. Calestani, G. Gigli, F. De Angelis, and R. Mosca, *Chem. Mat.* **25,** 4613 (2013).

[20] R. J. Elliott, *Phys. Rev.* **108**, 1384 (1957).